Possibility of Superconducting and Other Phases in Organic High Polymers of Polyacene Carbon Skeletons. I. Screened Electron-Electron Interaction—Random Phase Approximation—

Minoru KIMURA,* Hiroyuki KAWABE,† Akihiko NAKAJIMA,† Kiyoshi NISHIKAWA,† and Shigeyuki AONO†
Department of Physics, Faculty of Science, Kanazawa University, Marunouchi, Kanazawa, Ishikawa 920
†Department of Chemistry, Faculty of Science, Kanazawa University, Marunouchi, Kanazawa, Ishikawa 920
(Received June 20, 1988)

The effective electron-electron interaction in the high polymers of polyacene carbon skeleton is investigated. The appearance of various phases in this system depends on associated parameters characterizing the electron-electron interactions near the Fermi level. The main purpose of this work is to estimate these parameters under the random phase approximation and to presume whether this polymer may or may not be superconductor at room temperature.

In studies of the high temperature superconductivity, many one- or two-dimensional models have been proposed and the probability of it was discussed.[1,2] We also studied, in our previous reports,[3,4] various phases of polyacene, especially its superconducting phase, which is quasi-one-dimensional system. We have stressed that a characteristic band structure near the Fermi surface of the present system leads to preferable properties to usual one-dimensional models in some points. For example, the gap and the transition temperature are proportional to the exponential of coupling constants in the BCS model for metal:[5]

$$\Delta = \omega_D \exp\left(\frac{-1}{\nu_F |g|}\right), \tag{1}$$

$$T_c = \omega_D \frac{\gamma}{\pi} \exp\left(\frac{-1}{\nu_F |g|}\right). \tag{2}$$

These are due to the linear dispersion of band structure near the Fermi surface. On the other hand, the quadratic dispersion of band structure in polyacene yields,[4]

$$\Delta = \frac{K^2}{4\pi^2 t} \lambda^2, \tag{3}$$

$$T_c = \frac{Z^2}{4t} \lambda^2, \tag{4}$$

where t is the transfer integral between adjacent sites, λ the characteristic parameter responsible for the phase transition (see Eq. 22), K and Z being the positive numerical factors of order 1 (the precise form is given in Ref. 4). The relations, (3) and (4) suggest that polyacene has a more extended region of superconducting phase than that in metal.

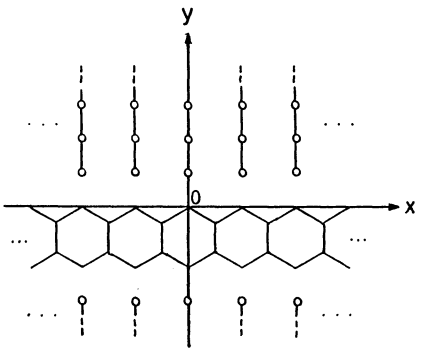

Fig. 1. Polyacene with side chains.

We have applied g-ology to our system, which parametrizes the interaction matrix elements near the Fermi momentum ($k=\pi$). In the present work, we estimate the g value numerically and wish to determine the phases of polyacene. In the BCS theory the superconducting phase occurs for negative g value, arising from the electron-phonon interaction. If the latter be replaced by any electronic process, even in the BCS superconductor, the Debye frequency in Eq. 2 is replaced by the associated electronic frequency, so that the critical temperature would be expected to be ten or hundred times larger. To make this be realized, we consider the system composed of the side chains attached to the both sides of polyacene skeleton (Fig 1). This is nothing but the idea proposed by Little.[8]

Single Particle States of Polyacene

We consider the transfer integral t between only the adjacent sites. In the case without bond alternation, the Hamiltonian is

$$H_0 = t\sum_n (a_{n1}^+ a_{n2} + a_{n2}^+ a_{n3} + a_{n4}^+ a_{n3} + \text{h.c.}) + t\sum_n (a_{n+1,1}^+ a_{n2} + a_{n+1,4}^+ a_{n3} + \text{h.c.}). \tag{5}$$

Here a_{nr}^+ (a_{nr}) is the creation (annihilation) operator of an electron at r-site of n-th unit cell (see Fig. 2). Because of the periodic property of polymer, the Born

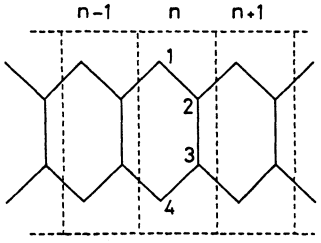

Fig. 2. Polyacene skeleton with the site and cell numbers.

von-Karman condition leads to

$$H_0=t\sum_k\{(1+e^{-ik})\,(a_{k1}^+a_{k2}+a_{k4}^+a_{k3})+a_{k2}^+a_{k3}+\text{h.c.}\},\qquad(6)$$

where, for example, a_{ki} is the Fourier transform of a_{ni}:

$$a_{ki}=\sum_n e^{-ikn}\,a_{ni}.\qquad(7)$$

The spectrum is composed of four bands given by

$$\begin{aligned}\varepsilon_{c'}(k)&=\frac{-t}{2}\{1+s(k)\}\ ,\\ \varepsilon_c(k)&=\frac{t}{2}\{1-s(k)\}\ ,\\ \varepsilon_v(k)&=\frac{-t}{2}\{1-s(k)\}\ ,\\ \varepsilon_{v'}(k)&=\frac{t}{2}\{1+s(k)\}\ ,\end{aligned}\qquad(8)$$

with

$$s(k)=\sqrt{9+8\cos k}\ ,\qquad(9)$$

and LCAO coefficients for atomic sites are

$$\|U_{rb}(k)\|=\begin{bmatrix}N_{c'} & N_c & N_v & N_{v'}\\ -N_{c'}\varepsilon_{c'}/\tilde{t}_k & -N_c\varepsilon_c/\tilde{t}_k & -N_v\varepsilon_v/\tilde{t}_k & -N_{v'}\varepsilon_{v'}/\tilde{t}_k\\ N_{c'}\varepsilon_{c'}/\tilde{t}_k & -N_c\varepsilon_c/\tilde{t}_k & N_v\varepsilon_v/\tilde{t}_k & -N_{v'}\varepsilon_{v'}/\tilde{t}_k\\ -N_{c'} & N_c & -N_v & N_{v'}\end{bmatrix},\qquad(10)$$

where

$$N_b^2=\frac{|\tilde{t}_k|^2}{2[|\tilde{t}_k|^2+\varepsilon_b^2]}\ ,\quad \tilde{t}_k^{-1}=\frac{e^{ik/2}}{2t\cos(k/2)}\ .\qquad(11)$$

In the above the column refers to the site, while the row to the level.

Instability

The interaction Hamiltonian H_{int} is written as

$$H_{\text{int}}=\frac{1}{4}\sum_{ijkl}\sum_{\alpha\beta\gamma\delta}\Gamma_{\alpha\beta\gamma\delta}^{ijkl}\,a_{i\alpha}^+a_{j\beta}^+a_{k\gamma}a_{l\delta},\qquad(12)$$

where Γ is the bare vertex part:

$$\Gamma_{\alpha\beta\gamma\delta}^{ijkl}=\langle i_\alpha j_\beta|k_\gamma l_\delta\rangle\delta_{\alpha\delta}\delta_{\beta\gamma}-\langle i_\alpha j_\beta|l_\delta k_\gamma\rangle\delta_{\alpha\gamma}\delta_{\beta\delta},\qquad(13)$$

with

$$\langle i_\alpha j_\beta\,|k_\beta l_\alpha\rangle=\int dr_1\,dr_2\,\phi_{i\alpha}^*(r_1)\phi_{j\beta}^*(r_2)V(r_1,r_2)\phi_{k\beta}(r_2)\phi_{l\alpha}(r_1)\,.\qquad(13a)$$

In order to consider the phase transition, we take into account only of v (the highest valence) and c (the lowest conduction) bands. Thus we obtain

$$\begin{aligned}H_{int}=\frac{1}{4}\sum_{p_1p_2p_3p_4}\delta(p_1+p_2,p_3+p_4)[&\Gamma_{\alpha\beta\gamma\delta}^{vvvv}a_{vp_1\alpha}^+a_{vp_2\beta}^+a_{vp_3\gamma}a_{vp_4\delta}\\&+\Gamma_{\alpha\beta\gamma\delta}^{vvcc}\,a_{vp_1\alpha}^+a_{vp_2\beta}^+a_{cp_3\gamma}a_{cp_4\delta}\\&+2\Gamma_{\alpha\beta\gamma\delta}^{vcvc}\,a_{vp_1\alpha}^+a_{cp_2\beta}^+a_{vp_3\gamma}a_{cp_4\delta}+(v\leftrightarrow c)].\end{aligned}\qquad(14)$$

Γ's are given by

$$\begin{aligned}\Gamma_{\alpha\beta\gamma\delta}^{vvvv}&=\Gamma_{\alpha\beta\gamma\delta}^{cccc}=g_1(\delta_{\alpha\delta}\delta_{\beta\gamma}-\delta_{\alpha\gamma}\delta_{\beta\delta}),\\ \Gamma_{\alpha\beta\gamma\delta}^{vvcc}&=\Gamma_{\alpha\beta\gamma\delta}^{ccvv}=g_2(\delta_{\alpha\delta}\delta_{\beta\gamma}-\delta_{\alpha\gamma}\delta_{\beta\delta}),\\ \Gamma_{\alpha\beta\gamma\delta}^{vcvc}&=\Gamma_{\alpha\beta\gamma\delta}^{cvcv}=g_3\delta_{\alpha\delta}\delta_{\beta\gamma}-g_4\delta_{\alpha\gamma}\delta_{\beta\delta},\end{aligned}\qquad(15)$$

with

$$\begin{aligned}g_1&=\langle vv|vv\rangle=\langle cc|cc\rangle,\\ g_2&=\langle vv|cc\rangle=\langle cc|vv\rangle,\\ g_3&=\langle vc|vc\rangle=\langle cv|cv\rangle,\\ g_4&=\langle vc|cv\rangle=\langle cv|vc\rangle.\end{aligned}\qquad(16)$$

Since two-body collisions near the Fermi surface play an important role, we have, in the above, constant matrix elements at the Fermi surface. For example, g_1 is given by

$$g_1=\int dr_1dr_2\phi_{vk_F}^*(r_1)\phi_{vk_F}^*(r_2)V(r_1,r_2)\phi_{vk_F}(r_2)\phi_{vk_F}(r_1)\,,\qquad(17)$$

where ϕ_{vk_F} is a single-particle wave function for the valence band at the Fermi surface. As will be seen in the following, electrons near Fermi level localize almost at the 1- or 4-site. Therefore it is expected that electrons passing along edges of skeleton are strongly influenced by the polarized side chains around the spine (see Fig. 1). When $k=k_F=\pi$, Eq. 10 leads for ϕ_{vk} and ϕ_{ck} to

$$\begin{aligned}\phi_{vk}&=2^{-1/2}(\chi_{k1}-\chi_{k4}),\\ \phi_{ck}&=2^{-1/2}(\chi_{k1}+\chi_{k4}),\end{aligned}\qquad(18)$$

where χ_{k1} is the Fourier transform of the Wanier function at site-1 of n-th cell. Namely,

$$\begin{aligned}\phi_{vk}&=(2L)^{-1/2}\sum_n(x_{n1}-x_{n4})\,e^{ikn},\\ \phi_{ck}&=(2L)^{-1/2}\sum_n(x_{n1}+x_{n4})\,e^{ikn}.\end{aligned}\qquad(19)$$

Moreover we neglect all differential overlaps. As a result, Eq. 17 turns out to be

$$\begin{aligned}g_1&=\frac{1}{(2L)^2}\int dr_1dr_2\sum_{m,n}V(r_1,r_2)\\&\quad\times[|x_{m1}(r_1)|^2+|x_{m4}(r_1)|^2][|x_{n1}(r_2)|^2+|x_{n4}(r_2)|^2]\\&=\frac{1}{(2L)^2}\sum_{m,n}(V_{m1,n1}+V_{m1,n4}+V_{m4,n1}+V_{m4,n4})\,.\end{aligned}\qquad(20)$$

Each matrix element depends on the difference, $m-n$, so that we give

$$\begin{aligned}g_1&=\frac{1}{2L}\sum_n(V_{01,n1}+V_{01,n4}),\\ g_2&=\frac{1}{2L}\sum_n(V_{01,n1}-V_{01,n4}),\\ g_3&=\frac{1}{2L}\sum_n(V_{01,n1}-V_{01,n4}),\\ g_4&=\frac{1}{2L}\sum_n(V_{01,n1}+V_{01,n4}).\end{aligned}\qquad(21)$$

Let us denote that[4]

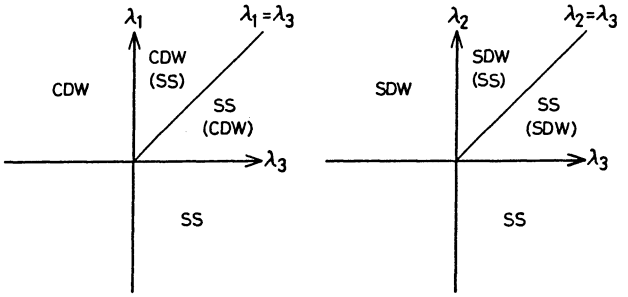

Fig. 3. Phase diagrams for polyacene.

$$\lambda_1 = -g_2 - 2g_3 + g_4,$$
$$\lambda_2 = g_2 + g_4,$$
$$\lambda_3 = -g_1 - g_2. \tag{22}$$

In the previous paper,[4] we have derived the phase diagram versus λ_1, λ_2, and λ_3 on the basis of simple mean field theory as shown in Fig. 3. Positive values of them correspond to appearance of CDW, SDW, and the singlet superconductivity (SS) phases, respectively. The figure suggests that the most possible ordered phase has the largest positive value of λ. Although the theory neglects the interference between various singular channels, we tentatively apply this result to the discussion about the model proposed by Little. In the following sections we calculate these parameters numerically.

Effective Interaction

The screening effect for the electron-electron interaction in the spine near the Fermi surface by electrons in the spine and in the polarized side chains is treated by the perturbation method as shown in Fig. 4. The double wavy line describes the effective interaction, $\tilde{V}_{\text{eff}}$, and the sigle wavy line the bare interation, V_{bare}. For V_{bare}, we adopt the Nishimoto-Mataga potential:

$$V_{\text{bare}} = \frac{14.40}{R_{rs}(n) + 1.33}\ (\text{eV}), \tag{23}$$

where $R_{rs}(n)$ is the distance from r-site of 0-th cell to s-site of n-th cell (in the unit of Å). The calculations were carried out using the following units: the bond length of benzene, 1.4 Å, for distances and the absolute value of the transfer integral, 2.5 eV, for energies. The shaded part of Fig. 4 displays the proper polarization part which includes various processes. We approximate it by the first two diagrams as shown in Fig. 4.

The Dyson equation for $\tilde{V}_{\text{eff}}$ is an integral equation in the coordinate space and is difficult to solve, but is easily manipulated in the momentum space. We take the Fourier transform of $V_{0r,ns}=V_{rs}(n)$ as

$$V_{rs}(n) = \frac{1}{L}\sum_k e^{ikn} v_{rs}(k) \tag{24}$$

and its inverse transform is

$$v_{rs}(k) = \sum_{n=-N}^{N} e^{-ikn} V_{rs}(n). \tag{25}$$

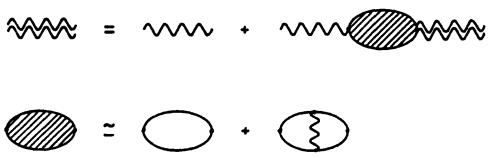

Fig. 4. The Dyson equation for electron-electron interaction and the approximation for the polarization part.

Thus the effective interaction is written in k pace as

$$\tilde{v}(k) = [1 - v(k)\Pi(k)]^{-1} v(k), \tag{26}$$

where $\tilde{v}$ and v are the effective and bare potentials, respectively. Note that each term is a matrix with respect to the atomic sites in the unit cell. We divide this into two parts, P and Q. The former refers to the spine and the latter to the side chain. Then Eq. 26 becomes[6]

$$\begin{bmatrix} \tilde{v}_{PP} & \tilde{v}_{PQ} \\ \tilde{v}_{QP} & \tilde{v}_{QQ} \end{bmatrix} = \left\{1 - \begin{bmatrix} v_{PP} & v_{PQ} \\ v_{QP} & v_{QQ} \end{bmatrix} \begin{bmatrix} \Pi_{PP} & \Pi_{PQ} \\ \Pi_{QP} & \Pi_{QQ} \end{bmatrix}\right\}^{-1} \begin{bmatrix} v_{PP} & v_{PQ} \\ v_{QP} & v_{QQ} \end{bmatrix}. \tag{27}$$

In order to proceed further, we assume $\Pi_{PQ}=\Pi_{QP}=0$, which implies that the charge transfer between the spine and the side chain is neglected, i.e., there is a single bond between them. Thus we get

$$\tilde{v}_{PP} = [1 - v_{PP}\Pi_{PP} - v_{QP}\Pi_{QQ}(1 - v_{QQ}\Pi_{QQ})^{-1} v_{QP}\Pi_{PP}]^{-1} \times [v_{PP} + v_{PQ}\Pi_{QQ}(1 - v_{QQ}\Pi_{QQ})^{-1} v_{QP}]. \tag{28}$$

If we restrict ourselves to retain the first order term with respect to Π_{QQ}, we get

$$\tilde{v}_{\text{Little}} = (1 - v_{PP}\Pi_{PP})^{-1} v_{PP} + v_{PQ}\Pi_{QQ}v_{QP}, \tag{29}$$

which is the Little's approximation.[6]

If we employ the random phase approximation for the proper polarization part, Π, which is given by the ring diagram in Fig. 4 and denoted by Π^0, it follows that

$$\Pi^0_{sr}(k, \omega) = 2\int \frac{d\nu}{2\pi i} \frac{1}{L}\sum_q G_{sr}(k+q, \omega+\nu) G_{rs}(q, \nu). \tag{30}$$

Using the representation diagonalizing the Hamiltonian (5) and carrying out the integration, we can get

$$\Pi^0_{sr}(k, \omega) = \frac{4}{L}\sum_q \sum_b^{un} \sum_{b'}^{occ} \frac{\langle s|b, k+q\rangle\langle b, k+q|r\rangle\langle r|b', q\rangle\langle b', q|s\rangle}{\omega - \varepsilon_b(k+q) + \varepsilon_{b'}(q)}. \tag{31}$$

In the above, we consider the symmetry property of each band to the Fermi surface. In carrying out the summation with respect to q we make a small cut-off around the Fermi momentum, because electrons in this small region are responsible for the instabilities associated with phase transitions.

In order to improve the random phase approximation for the polarization part, we take into accout the oyster diagram, the second one in the right hand side

of Fig. 4. This involves four Green's functions in the integral the calculation of which requires enormous machine time. Then we are obliged to use an approximation in which the bare electron-electron interaction is restricted only to the one-center type. Thus we get

$$\Pi^{1}_{sr}(k) = \frac{-1}{2}\sum_{t}\Pi^{0}_{st}(k)v_{tt}(k)\Pi^{0}_{tr}(k)\,. \qquad (32)$$

It is said that this approximation amounts to 70—80% of the full contribution.[8]

In the following, we use the static approximation, as with $\omega=0$ in Eq. 31.

Side Chain

Since, in the present case, the polarization of the side chain plays a role of the phonon part in the ususal superconductor, it is crucial to choose a suitable side chain. We proceed our consideration along the Salem's idea.[9]

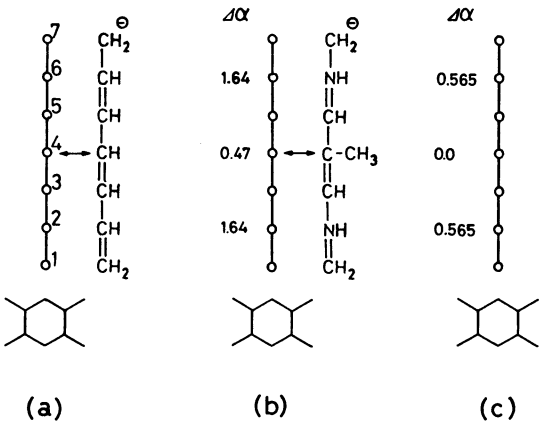

Fig. 5. Side chains. $\delta\alpha_s$ is given in the unit t. (a) Unoptimized, (b) optimized by Salem, and (c) optimized perturbatively.

As the simplest case, we take a dye molecule which is, as shown in Fig. 5a, a conjugated hydrocarbon with eight π-electrons and seven atomic sites. In this molecule, the polarization spreads all over the molecule, so that it is not so effective to reduce the electron-electron interaction on the spine. In order to make it efficient, one can introduce some substituents. Due to the well known symmetry properties of the alternant hydrocarbon, the nonbonding molecular orbital, say the 4-th one in this case, has vanishing amplitude on the even-numbered sites (called the unstarred sites). Even if we put substituents on these sites, this orbital is not affected. Therefore we can design these substituents so that the transition amplitude to the next higher level, which is expected to be most effective for polarization, shall be considerably small except for the both molecular ends.

Following this idea, Salem has obtained the one shown in Fig. 5b, exactly in the frame-work of the Hückel theory. Note that this is not unrealistic from the experimental view-points.

What mentioned above is well understood by the elementary perturbation theory, too.[7] A small perturbation at s-th site, $\delta\alpha_s$ changes the amplitude, $\langle r|i\rangle$ to $\langle r|\tilde{i}\rangle$ as

$$\langle r|\tilde{i}\rangle = \langle r|i\rangle + \sum_{j,s}\frac{\langle r|j\rangle\langle j|s\rangle\delta\alpha_s\langle s|i\rangle}{\varepsilon_i - \varepsilon_j}\,, \qquad (33)$$

where r refers to the site except the two ends, s to unstarred one and i to the lowest vacant level. The optimizing condition for the substituents is found by putting the left hand side of Eq. 33 equal to zero. The coditions obtained by the perturbation analysis are more general but less accurate than the Salem's ones. $\delta\alpha_4=0$ at the beginning, then we obtain a result given in Fig. 5c.

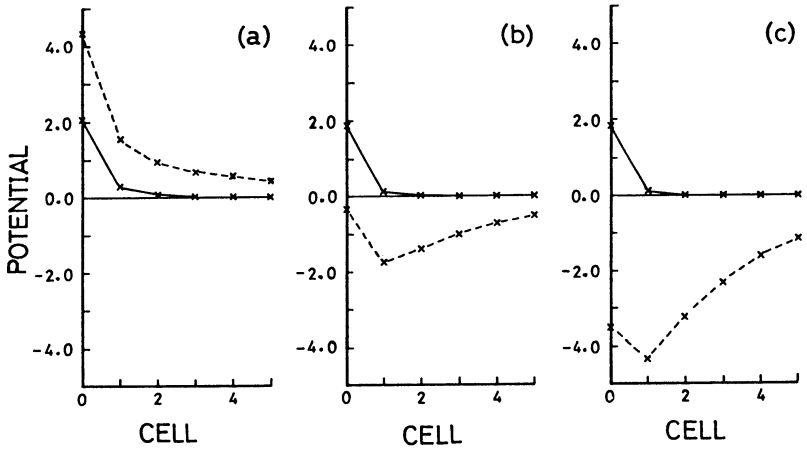

Fig. 6. The screened potential for various cases. (a) Only the spine. Dotted line is for the bare interaction and the solid line for the screened one. (b) The spine with unoptimized side chains. (c) The spine with optimized side chains by Salem. In the cases of (b) and (c), the dotted lines refer to the Little's approximation, and the solid ones to ours. For all cases, the cut-off is 0.01.

Results and Discussion

We should like to mention a little about the numerical procedures. Our final object is to get the coupling constants g_1—g_4. Since these (see Eq. 21) are the components with $k=0$ in the momentum representation, we can get them as the simple sums of coupling constants in the space representation, of course, the latters being renormalized. Suppose that we use two hundred cells in the practical calculation. Since each cell contains four atomic sites, the procedure for getting the screening effect becomes a problem of 800×800 matrix manipulation. This is considerably tedious. In the momentum space, one needs 200 4×4 matrix manipulations. In order to evaluate each term in the right hand side of Eq. 21, the inverse-Fourier transform is used.

The values of $V_{1,1}(n)$ thus obtained are shown in Fig. 6. In Fig. 6a, the screened potential (the solid line) decays very fast and becomes almost zero at the next neighbor cell. This result contrasts with that obtained by Schug et al.[10] They calculated the screened potential for $C_{57}H_{59}$ molecule only within the random phase approximation and obtained the potential which is screened in short-range region but is enhanced in long range region. This shows that for the screening effect in conjugated molecules the Π^1 effect is impotant as well as the Π^0 one. The Little's approximation (dotted lines in Figs. 6b and c) tells us that the side chain works very well to get attractive interactions, while in our higher approximation (solid lines) the potential is not attractive. The modification for the side chain does not affect the behavior qualitatively.

The above trends are shown in more detail in Table 1. It is noted that results are almost independent of cut-off parameters. In the table, every case has two lines, the upper is carried out by including Π^0 only, while the lower by including Π^0 and Π^1. The Π^1 effect is not so significant. Look at the final group. Little's approximation suggests the spine be superconducting at 900 K or higher. But our more elaborate calculation denies his conclusion. As to the side chain effect, the first order effect which is described by the Little's approximation for the polarization part in the side chain gives a considerable effect to the spine, but the higher order effects which are something like the back flows, cancel the first order effect.

We have made several trials for the shape of the side chains, e.g., some networks of the above mentioned side chains, which are constructed by introducing appropriate transfers between them. However, everything has been in vain to make the potential attractive.

Finally, our result is shown in Table 2 for the case of the spine with unoptimized side chains (other models also give qulitatively the same results.). Present result predicts that the SS state is not likely since $\lambda_3<0$ and the SDW state is more favorable than the CDW state since $\lambda_2>\lambda_1$.

Table 2. The Coupling Parameters

g_1	g_2	g_3	g_4	λ_1	λ_2	λ_3
0.059	0.004	0.004	0.059	0.046	0.063	−0.063

These are calculated for the case of the spine with unoptimized side chains. For the treatment of the side chain polarization, of course, ours is adopted. The cut-off parameter is 0.010.

Table 1. Possibility of Superconducting State

Model		Cut 0.005 λ_3	0.005 T_c	0.010 λ_3	0.010 T_c	0.015 λ_3	0.015 T_c
Only spine		−0.037		−0.038		−0.038	
		−0.068		−0.070		−0.070	
Spine with unoptimized side chain	Little	0.313	401	0.312	400	0.312	400
		0.284	364	0.283	363	0.283	363
	ours	−0.033		−0.034		−0.034	
		−0.062		−0.063		−0.063	
Spine with optimized side chain (perturbative)	Little	0.474	607	0.473	606	0.473	606
		0.452	579	0.451	578	0.451	578
	ours	−0.033		−0.034		−0.034	
		−0.062		−0.063		−0.063	
Spine with optimized side chain (Salem)	Little	0.735	941	0.734	940	0.734	940
		0.724	927	0.722	926	0.722	926
	ours	−0.033		−0.034		−0.034	
		−0.061		−0.063		−0.063	

Data of λ_3 and T_c for various models and cut-off parameters. (1) Only the spine. (2) The spine with unoptimized side chains. (3) The spine with side chains optimized perturbatively. (4) The spine with side chain optimized by Salem. Each case is separated into two treatments: Little's approximation and ours. Every one has two lines, the upper in carried out by including Π^0 only, while the lower by including Π^0 and Π^1. The unit for cut and λ_3 is t, and that for T_c is degree.

References

1) "Highly Conducting One-Dimensional Solid," ed.by J. T. Devreese, R. P. Evrard, and V. E. van Doren, Plenum, New York (1979).
2) V. L. Ginzburg, *Ann. Rev. Mater. Sci.*, **2**, 663 (1968).
3) M. Kimura, H. Kawabe, K. Nishikawa, and S. Aono, *J. Chem. Phys.*, **85**, 3090 (1986).
4) M. Kimura, H. Kawabe, K. Nishikawa, and S. Aono, *J. Chem. Phys.*, **85**, 3097 (1986).
5) J. R. Schrieffer, "Theory of Superconductivity," Benjamin, New York (1964).
6) W. A. Little, *Phys. Rev.*, **134**, A1415 (1964).
7) J. Yoshida, K. Nishikawa, and S. Aono, *Prog. Thoret. Phys.*, **50**, 830 (1973).
8) H. Gutfreund and W. A. Little, *Phys. Rev.*, **183**, 68 (1969).
9) L. Salem. *Mol. Phys.*, **11**, 499 (1966).
10) J. C. Schug, R. D. Reid, A. C. Lilly, and R. W. Dwyer, *Chem. Phys. Lett.*, **128**, 5 (1986).